

MARSHALL GRANT

IN-76-CR

122401

P-29

**FINAL REPORT**

NASA GRANT NAG8-868

**FNAS/ADVANCED PROTEIN CRYSTAL GROWTH**

Period of Performance  
3/11/91 through 9/10/92

Principal Investigator  
FRANZ ROSENBERGER

(NASA-CR-190910) FNAS/ADVANCED  
PROTEIN CRYSTAL GROWTH Final  
Report, 11 Mar. 1991 - 10 Sep. 1992  
(Alabama Univ.) 29 p

N92-34170

Unclass

63/76 0122401

Center for Microgravity and Materials Research  
University of Alabama in Huntsville  
Huntsville, Alabama 35899

**Temperature dependence of protein solubility - Determination and application to crystallization in x-ray capillaries**

F. Rosenberger, S. B. Howard, J. W. Sowers and T. A. Nyce

*Center for Microgravity and Materials Research, University of Alabama in Huntsville, Huntsville, Alabama 35899, U. S. A.*

Received            June 1992

**Abstract**

A scintillation method is presented for determination of the temperature dependence of the solubility,  $S(T)$ , of proteins in 50-100  $\mu\ell$  volumes of solution.  $S(T)$  data for lysozyme and horse serum albumin were obtained for various combinations of pH and precipitant concentrations. The resulting kinetics and equilibrium information was used for dynamic control, that is the separation of nucleation and growth stages in protein crystallization. Individual lysozyme and horse serum albumin crystals were grown in 15-20  $\mu\ell$  solution volumes contained in x-ray capillaries.

## 1. Introduction

Decades of research on the growth of inorganic crystals from solutions has shown that high structural quality and uniformity in composition can only be achieved if growth is conducted slowly and steadily. High growth rates, as well as seemingly small variations in growth-driving conditions, are prone to result in defect formation, such as the enhanced formation of dislocations at growth sector boundaries and the occlusion of mother liquor in growth striations or bands. An extreme example is the formation of growth bands in ammonium dihydrogen phosphate in response to growth temperature changes as low as  $10^{-2}$  °C [1]. Protein crystals intrinsically grow much slower than most inorganic crystals at the same supersaturation. This is probably one of the reasons why it has been widely believed that steadiness and, hence, close control of the growth conditions, are not as important for crystal perfection in protein crystallization. Recently, however, we have shown that there is also a one-to-one correspondence between changes in growth conditions and defect formation in lysozyme [2]. Changes in the growth temperature of only a few tenths of a degree resulted in macroscopic solution occlusions. Furthermore, relatively high growth rates ( $10^2$  Å/s) led to an increase in structural defect density, while low growth rates led to their decrease [2].

These observations corroborate the expectation [3,4] that close control of growth conditions is as important for the growth of highly perfect protein crystals as it is for inorganic crystals. Such close control includes means to restrict nucleation events to a few at the beginning of a crystallization run. Since the pioneering works of Ostwald [5] and Miers and co-workers [6] it has been known that the formation of a solid nucleus within a melt or solution requires a considerably higher undercooling or supersaturation than the growth onto a solid in contact with the same nutrient. A more recent solution growth example for this general behavior is given in [7]. Hence, in inorganic crystal growth it is common practice to either homogeneously or heterogeneously seed solutions at supersaturations that are too low to drive bulk nucleation. Or, if no single crystalline seeding material is available, the supersaturation is rapidly lowered below the

nucleation threshold after the onset of bulk nucleation. Failure to impose such dynamic control results in concurrent formation of new nuclei and, often, too rapid growth of the initial nuclei. This, in turn, leads typically to interference of the crystallites either through the solute field or through mechanical contact and overgrowth.

Seeding of homoepitaxial growth has been successfully performed by various protein crystal growers; for examples see [8,9]. For seed transfer from mother solutions, it should be noted that small differences in the salt concentration of the solutions in which a seed is nucleated and into which it is transferred for further growth, were found to lead to growth cessation [10]. Heteroepitaxial seeding and growth of proteins on mineral substrates has also been reported [11]. Most recently, some protein single crystals were obtained through graphoepitaxy [12].

Supersaturation reduction after initial nucleation, on the other hand, is not typically provided for in most current protein crystal growth procedures [13,14]. Only the dialysis or interdiffusion technique possesses some limited internal means toward this end. During dialysis of the initially separated salt (precipitant) and protein solutions, the concentration gradient and, thus, the exchange rate across the membrane, decrease with time. Hence, the initial high supersaturation in the protein solution at the membrane also decays with time, frequently resulting in fewer crystals than are obtained with other techniques. Toward external supersaturation control, experiments were made to regulate the humidity content of a gas flow over a hanging drop in the vapor diffusion technique [15].

Of the many parameters used to drive the nucleation and crystallization of macromolecules (see, e.g., Table III in [14]) few are technically suitable for supersaturation control. Of these, temperature control is particularly attractive [16] because a) heat diffuses in aqueous solutions at least two orders of magnitudes more rapidly than species, b) it can easily be applied to closed systems, and c) precise temperature control and programming technology is readily available.

Crystallization of proteins by temperature lowering (with systems of normal solubility) is cited as early as 1881 [17] and 1892 [18]. In 1949, saturated protein solutions sealed into glass

capillaries were cooled at rates of 1 °C/hr or less to produce gramicidin S crystals [19,20]. Solutions are often produced at room temperature and then stored in a refrigerator to induce nucleation, see, e.g., [21,22]. Protein solutions were even briefly brought to -20 °C and then rewarmed to 5 °C to induce nucleation within hours rather than the days needed at the higher temperature [23]. Note that the last example includes supersaturation reduction after a nucleation stage. A few workers have taken advantage of temperature gradients for protein crystallization [24]. Protein systems with retrograde solubility, typically associated with high salt concentrations [25-27], have been correspondingly warmed to induce crystallization [28,29]. A particularly complex system was investigated in [30]: a pure enzyme showed retrograde solubility, but crystals of a complexed form were obtained by temperature lowering, that is they possessed normal solubility.

The above examples utilizing temperature *changes* are presented to illustrate the various scenarios of protein crystallization. Many more can be found in the literature, see [13,14,31]. Very few investigators, however, have emphasized the need for temperature *control and programming* to separate nucleation and growth stages. In our group, a thermostatted solution growth cell with localized cooling provided by a growth sting was used to grow crystals of both lysozyme and equine serum albumin [32]. The jacket and sting temperatures were controlled independently and a radial temperature gradient was established on the sting. The initial nucleation was restricted to the central region of the sting. Appropriate temperature programming prevented further nucleation and reduced the number of initial nuclei (crystallites) to inhibit interference. Other researchers have also been successful in localizing and limiting the number of nuclei in a similar arrangement [33]. Because these growth cells require solution volumes of the order of ml and, thus, are not applicable to less readily available proteins, we have miniaturized this technique. Its final configuration and application to the growth of proteins from 15-20  $\mu\ell$  solutions in x-ray diffraction capillaries will be described below.

The optimization of a temperature program for the nucleation and growth of a specific protein requires data on the temperature dependence of its solubility,  $S(T)$ , at the salt

concentration and pH to be used in the crystallization experiments. To date, systematic studies of protein solubilities have been limited to tetragonal and orthorhombic lysozyme [34-39], concanavalin [40], and concanavalin A [41]. This scarcity of S(T) data for proteins is partly due to the relatively large volumes required by the earlier solubility determination techniques [34-37, 40]. Recently, however, micro-techniques were employed that utilize a novel micro-column method [38,39], the removal of supernatants from small drops in which crystals grew [41], or an optical scintillation technique developed in our group [16]. Hence, solubility data can now be readily gathered for proteins that are available only in limited quantities. The scintillation technique and its application to determinations of the S(T) of tetragonal lysozyme and horse serum albumin, involving carefully prepared solutions (Section 2) is described in Section 3. The application of these S(T) data to temperature-controlled growth in x-ray capillaries is presented in Section 4.

## 2. Solution preparation

### 2.1 *Hen egg-white lysozyme*

Lysozyme chloride from chicken egg-white (Grade VI, L2879, 90% protein, 10% buffer salts) was purchased from Sigma Chemical Company. The as-received protein was dissolved at room temperature in deionized and Millipore-filtered (0.22  $\mu\text{m}$ ) ultra pure biological type-1 water ( $\text{diH}_2\text{O}$ ). The solution was filtered with a sterile Nalgene filter with an average pore size of 0.2  $\mu\text{m}$ .

Because as-received protein can vary in composition between batches, we performed analytical SDS-PAGE (sodium dodecyl sulfate-polyacrylamide gel electrophoresis) to characterize the purity of lysozyme. In all cases, using either Coomassie Blue or silver staining, only one band was obtained at molecular weight  $\approx 14,500$ .

In order to establish a well-defined salt concentration in the growth solutions, all salt present in the as-received lysozyme was removed. For this, the filtrate was placed in dialysis tubing (molecular weight cutoff  $\approx 8,000$ ) and dialyzed against deionized water for about 30 hours with at least two changes of  $\text{diH}_2\text{O}$ . In previous experiments with NaCl solutions of known

concentrations, using a  $\text{Na}^+$  specific electrode, we found that in our apparatus two complete water changes in 25 hours were sufficient for quantitative salt removal.

The protein was then dialyzed for a total of 60 hours against 0.05M acetate buffer at pH = 4.5, with 0.01 (w/v)%  $\text{NaN}_3$  added to inhibit microbial growth. The buffer solution in the reservoir was periodically replaced. After the dialysis, the lysozyme solution was filtered through a 0.2  $\mu\text{m}$  Nalgene filter, and then concentrated to approximately 110 mg/ml of solution using an Amicon ultrafiltration apparatus. The pH of this protein stock solution was checked with an Orion SA 520 pH meter. Lysozyme stock solutions were stored at 4 °C. In addition, stock solutions of 10 (w/v)% NaCl in 0.05 M acetate buffer of pH = 4.5 with 0.01 (w/v)%  $\text{NaN}_3$  were stored at 4 °C.

Final solution samples were prepared at room temperature by adding volumes of the stock solutions of protein and salt, and buffer to obtain the desired concentrations. These volumes were delivered with Eppendorf pipettes, which have precision and accuracy for the viscous protein solutions of  $\pm 0.4\%$  and  $\pm 1.2\%$ , respectively. These were determined through weighing a large number of delivered volumes. The salt solution was added last and the sample was immediately vortexed to ensure thorough mixing of the components. The solution was then centrifuged at 9,000 rpm in a Savant microcentrifuge to remove any particulate matter. The supernatant was then pH-corrected to pH = 4.5 using either glacial acetic acid or sodium acetate, analyzed for final protein concentration (see below) and transferred through syringes with 0.2  $\mu\text{m}$  filters into the scintillation cells or capillary growth tubes.

The protein concentrations in the stock and final solutions were determined by UV absorbance measurements at 280 nm with a Beckman DU-68 spectrophotometer. The concentration of lysozyme was calculated using Beer's Law,  $A = \alpha \ell C$ , where A is the absorbance (the natural logarithm of the ratio of impinging to transmitted intensity),  $\alpha$  is the absorption coefficient,  $\ell$  is the pathlength [cm], and C is the concentration [mg/ml]. We used  $\alpha_{280\text{nm}} = 2.64$  [ml/(mg cm)] for the absorption coefficient [42], and carried out multiple absorbance readings to increase confidence in the sample concentrations.

## 2.2 Horse serum albumin

Horse serum albumin (also referred to as equine serum albumin, ESA) was obtained in powder form from Sigma Chemical Company (A5280, Cohn's Fraction V, essentially fatty acid free, 99 % albumin). The precipitant and pH conditions chosen (40-50 (w/v)% ammonium sulfate, pH = 5.5) were found advantageous for single crystal growth by other workers [43]. Note that these precipitant concentrations are much higher than in the lysozyme system.

The preparation of stock solutions containing 150-200 mg/ml ESA, with 0.05 M acetate buffer at pH = 5.5 and 0.01 (w/v)% NaN<sub>3</sub>, followed essentially the procedure described above for lysozyme, without the salt removal step. The purity of the as-received protein was again checked by SDS-PAGE, and by isoelectric focusing. The three most probable contaminating proteins are the  $\alpha$ -,  $\beta$ -, and  $\gamma$ -globulins with isoelectric points at pH = 4.9, 6.3, and 6 to 7, respectively [44]. The published isoelectric point for equine serum albumin is pH = 4.9 [44]. Some multiple bands were seen between pH = 4.5 to 5.3, possibly indicating the presence of  $\alpha$ -globulin. However, the molecular weight determinations clearly showed single bands around ESA's reported molecular weight of 67,500 [45], but no bands around the molecular weight of  $\alpha$ -globulin of approximately 147,000 [46]. Thus, we concluded that the ESA was essentially free from contaminating proteins, and that the multiple banding was due to the well-known microheterogeneity of the albumin itself [47].

ESA stock solutions of 0.05 M acetate buffer at pH = 5.5 with 0.01 (w/v)% sodium azide added to inhibit microbial growth were stored at 4 °C for no more than two weeks. Longer storage can lead to significant increases of the microheterogeneity of ESA [48]. Saturated ammonium sulfate solutions (61.2 g ammonium sulfate, 100 g pH = 5.5 buffer) were stored at room temperature to prevent crystallization.

To our knowledge, absorption data for ESA, needed for optical concentration determinations, had not been reported before. Hence, we determined the UV spectrum and calibrated the absorbance as a function of concentration. Fig. 1 shows, for a solution containing 1.79 mg/ml ESA, that the absorption has a maximum at 276 nm, with an absorbance of 0.725.

Fig. 2 presents the absorbance at this wavelength obtained for solutions of various concentrations. The straight line was derived from these data with a correlation coefficient of 1.00, thus confirming Beer's law behavior. The slope of the line, i.e. an absorption coefficient of  $\alpha^{276\text{nm}} = 0.404$ , was used for our concentration determinations.

### 3. Solubility measurements

#### 3.1 Apparatus and procedures

Fig. 3 presents an exploded view of the scintillation arrangement used in our solubility studies. Between 50-100  $\mu\text{l}$  of solution are contained in a jacketed silica micro-cell (Wilmad Glass Co., model WG-65-Q-1) which is connected to a programmable constant temperature ( $\pm 0.1$  °C) recirculator bath (Polyscience, model 90). A laser beam from a self-contained laser diode assembly (MWK Industries, model CN 12, 5 mW) is directed through the solution. Light scattered normal to the beam is detected by a photodiode (United Detector Technology, model UDT 455) through a solid glass ground joint that seals the port of the cell, thus preventing evaporation of solvent. The temperature of the solution is monitored with a glass-bead thermistor (not shown) that is inserted through a groove in the ground joint. A beam splitter (Edmund Scientific, stock number A 32,601) between laser and cell diverts some of the laser's output to a second photodiode, the signal of which is used to compensate for intensity fluctuations in the impinging light. Backscatter of light that passes through the cell is minimized by a beam stop or light trap consisting of black fabric in a cavity formed by a rotating magnet. This magnet (Magnetic Fabricators, model AM-306-RH) drives a small nickel wire (0.6 mm diameter and 7 mm long) used as a stirring bar inside the lower part of the solution which is not illuminated by the laser beam. The cell and the laser/beam-splitter housing are held in place by five rectangular Plexiglas parts, see fig. 3, which require only three bolts (not shown) for their assembly. The whole assembly, together with a stirring motor (Hurst Mfg., model T-ET P/N 2609-001, 300 rpm), is housed in a light-tight metal can. The output of the two photodiodes and the thermistor are fed to a Macintosh computer via a MacADIOS Model 411 interface for data acquisition and

display. In turn, the temperature of the recirculator bath is programmed from the computer through this interface according to the changes in scintillation signal with time, see below.

A solubility point is determined as follows. After filling the cell with a solution of predetermined composition, the bath temperature is lowered (or raised in retrograde solubility systems) to a value at which nucleation and crystallite growth are expected to set in after some reasonable length of time, causing a distinct increase in the photodiode signal. Then the temperature is raised. Fig. 4 displays the temperature changes, imposed manually in this first transient, and the corresponding photodiode output (scintillation signal) in a run with a solution containing about 50 mg/ml of lysozyme and 2.5(w/v)% NaCl. The low background in the diode signal is the result of reflections from some sub-micron particulates and from the cell surfaces. One sees that, in spite of about 20-fold supersaturation of this solution at the low temperature of 7 °C (see fig. 6), the formation of crystallites requires about one hour. Note that at 10 °C this requires about 6 hours, well illustrating the exponential dependence of nucleation rates on supersaturation. Interestingly, the scintillation signal increases for some time even after the temperature is reset to a higher value (20 °C in fig. 4). This reflects the coarsening of the crystallites during this period.

After the manually controlled initial nucleation stage, the temperature is automatically increased in increments of 0.5 or 1 °C by the computer. Fig. 5 shows a temperature trace with corresponding scintillation signal levels for a lower concentration solution; for details see figure caption. In this run the scintillation light level was so high that the photodiode became saturated. When the solubility temperature is approached, the signal begins to drop due to sufficient dissolution of some of the crystallites. At a given temperature T the signal tends to level-off corresponding to the concentration of remaining crystallites that are in equilibrium with the solution at T. In order to save measurement time, however, the temperature is automatically changed by another increment as soon as the slope of the scintillation signal curve falls below a prescribed value. Hence the scalloped shape of the curve. When all crystallites have dissolved, the signal returns to the baseline. At the endpoint a small amount of solution is extracted from the

cell through a microsyringe with filter (Millipore Acrodisc, 0.2  $\mu\text{m}$  pore size) for optical concentration determination after appropriate dilution. Of course, the endpoint can be shifted to higher values by the formation of significant amounts of denatured proteins. This, however, can be recognized by the absence of a scallop on further temperature lowering.

The stirring of the cell solution serves several purposes. Foremost, it keeps the crystallites in suspension, which otherwise would sediment and not contribute to the scintillation signal. Stirring also expedites the nucleation process and the equilibration between crystallites and solution. This and the semi-automation of the procedure are essential in view of the slow kinetics involved.

### 3.2 *Lysozyme solubilities*

We have determined the temperature dependence of lysozyme solutions at 2.1 (w/v)%, 2.5 (w/v)%, and 3.0 (w/v)% NaCl and pH = 4.5. The results, presented in fig. 6, reflect normal solubility behavior, as well as the widely-occurring trend of decreasing solubility with increasing salt concentration, - salting-out behavior [49]. The solid lines correspond to third order polynomial fits, with the coefficients and average deviations listed in table 1. The dashed lines represent the results obtained by Pusey et al. at 2.0 (w/v)% and 3.0 (w/v)% NaCl with the equally rapid microcolumn technique [39]. In the range where the conditions overlap, the data agree well. Furthermore, the 2.5 (w/v)% data were nicely confirmed in kinetics studies in which lysozyme crystals under conditions slightly to the left or right, respectively, of the middle curve in fig. 6 clearly grew or etched [2].

Note, however, that our solubilities are considerably lower than those obtained with the batch method [34]. Batch methods, due to their essentially diffusion-limited equilibration of large volumes, require stable conditions over periods as long as ten months. Over such long periods it is difficult to keep the temperatures constant (power failures!), and to prevent microbial contamination and leakage of the solutions. Another problem with the lysozyme batch data appear to have arisen from the coexistence of tetragonal and orthorhombic crystals forms. Orthorhombic crystals, more stable than the tetragonal at the higher temperatures, possess lower solubilities.

Thus, subject to the equilibration kinetics of the two forms, the superposition of the different solubility curves can lead to the previously reported solubility maximum [34]; for more details see [32]. In the scintillation investigations, only the tetragonal form was present because orthorhombic crystals require longer periods to form.

### *3.3 Horse serum albumin solubilities*

Solubilities for equine serum albumin were obtained at 45 wt%, 47 wt%, and 51 wt% ammonium sulfate and pH = 5.5. In comparison with the lysozyme studies, the ESA solubility measurements required significantly longer experiment times due to slower dissolution kinetics. The results are displayed in fig. 7 and reflect the retrograde solubility behavior qualitatively observed by McMeekin in 1939 [45]. The solid lines correspond to fifth-order polynomial fits, with the coefficients and average deviations listed in table 2. Unexpectedly, the data show first a salting-out and then salting-in behavior with increasing ammonium sulfate concentration. This and the relatively large scatter in data prompt us to view these results with some reservation.

### *3.4 Canavalin solubilities*

Canavalin studies are discussed here to illustrate some limitations of the scintillation technique and, correspondingly, of the temperature control of crystallization. Canavalin was isolated from jack bean meal (Sigma J-0124, Lot 37F-3720) using the isolation procedure of Smith et al. [50]. Canavalin was also obtained from Prof. A. McPherson, University of California at Riverside. Details of the preparation of the 1.3 (w/v)% NaCl solutions used are given in [32]. Canavalin solubility was initially believed to have a strong temperature dependence. However, the nucleation response was so slow that, even with seeding, a typical canavalin experiment required 3-5 days to complete. In addition, the scintillation signals usually remained below 15% of the response obtained with lysozyme and ESA.

In batch crystallizations we found that, as had been observed earlier [50,51], in the solutions where crystals formed, the pH had increased significantly. Even though buffered at an initial pH of 5.5, the pH of our solutions was found to increase up to as 6.6. Further experiments

suggested, in agreement with findings of others [52], that the solubility of canavalin depends more on pH than on temperature. Thus we concluded that, under the solution conditions used, canavalin is a poor candidate for temperature controlled crystallization [32].

#### 4. Crystal growth in x-ray capillaries

The major advantages of protein crystallization in x-ray capillaries are that only small solution volumes are required and potentially damaging crystal handling between growth and diffraction studies can be avoided; for more details see [53]. An additional advantage of thin-walled capillaries is that heat flow in the wall in axial directions is minimal. Hence, temperature changes to induce nucleation by external means can be highly localized. In the following, we describe our experimental setup and procedures used for the growth of single crystals of lysozyme and ESA.

##### 4.1 Apparatus and loading

Fig. 8 presents a cross-sectional view of our growth apparatus. An x-ray capillary (Charles Supper Co, Glaskapillaren) containing 15-20  $\mu\ell$  of protein solution, rests on one side on a small tapered copper block which is in good thermal contact with a miniature thermoelectric (Peltier) heat pump (Marlow Industries, model MI 1021T). The temperature of the copper block is monitored with a bead thermistor (Marlow, model tH1) which also provides the signal for a temperature controller (Marlow, model SE 5010) that powers the heat pump. The lower side of the Peltier unit is in thermal contact with a heat conductor that rests on the inner wall of double-walled thermostatted glass jacket. Depending on the mode of operation of the heat pump, the heat conductor and glass jacket act as heat sink or source. With this arrangement the temperature of the copper block and, thus, of the spot of the capillary wall that is in contact with the block, can be programmed between 8 °C and 50 °C with a resolution of  $\pm 0.1$  °C. Similarly, the jacket, which is thermostatted by a programmable constant temperature recirculator bath (Neslab, model RTE 100) maintains the temperature of the remainder of the capillary to within  $\pm 0.1$  °C at some (other) predetermined value. Tight sealing of the jacket with a rubber stopper, which serves also as

feedthrough for the various lead wires, is important to prevent condensation of moisture on the heat pump at sub-ambient operation. The air inside the jacket is dried by some silica gel beads (not shown) to ensure safe heat pump operation and good viewing of nucleation and growth through a Wild long focal length microscope.

Capillary tubes were cleaned with an enzymatic action detergent and concentrated sulfuric acid, then thoroughly rinsed with filtered deionized water, and dried in a vacuum oven at  $\sim 120$  °C for several hours. After sealing one side with a quick-setting epoxy, the capillary was charged with the solution through a microsyringe and sealed on the other side.

#### 4.2 *Crystal growth*

Fig. 9 shows a lysozyme crystal (0.8 mm x 0.9 mm) grown in the above arrangement and photographed through the x-ray capillary, the edges of which correspond to the upper and lower edges of the photograph. The initial solution composition was 50 mg/ml, 3 (w/v)% NaCl and pH = 4.5; see the right curve in fig. 6. Nucleation of one crystal was observed 45 min after cooling the copper block to 7 °C, while the jacket was set to 32 °C. Immediately after nucleation was detected, the copper block temperature was increased to 19 °C, where the crystal shown in fig. 9 grew within 16 hrs.

The growth of only one crystal in the above run was somewhat fortuitous. However, we have always succeeded in limiting the number of crystals to 1-3 in all other runs by raising the "cold spot" temperature to the growth temperature even before the appearance of a macroscopic crystallite, thus reducing the chance for the successive formation of nuclei. Guidance for an advantageous choice of the nucleation induction time can be obtained from the initial transient time in the scintillation experiments; see fig. 4. One must take into account, however, that in these experiments multiple nucleation is desirable. Hence, one will chose somewhat lower supersaturations for the growth runs.

For the growth of ESA crystals, according to their retrograde solubility (fig. 7), the copper block temperature must be increased. Fig. 10 depicts an ESA crystal (0.94 mm x 0.06 mm) that was grown from a solution of initial 40 mg/ml protein concentration at pH = 5.5 and 45 wt% of

ammonium sulfate. Nucleation occurred after 2 hrs at 26 °C, and growth was conducted at 20 °C for about 200 hrs. The jacket temperature was kept at 19 °C throughout.

## **5. Conclusions**

The scintillation technique presented here is well suited for determination of the temperature dependence of the solubility of proteins in 50-100  $\mu\ell$  volumes of solution. The kinetics and equilibrium information gained from such determinations can be readily used for the dynamic control, i.e. the separation of nucleation and growth stages, in protein crystallization. X-ray capillaries can be advantageously used in temperature-controlled solution growth of individual protein crystals.

## **Acknowledgements**

Support of this research by NASA under grants NAG8-711, NAG8-824 and NAG8-868, and by the State of Alabama through the Center for Microgravity and Materials Research are gratefully acknowledged. We also want to thank Mike Banish for help with the photodiode circuitry, Lynne Carver for preparing the figures, and Melissa Rogers for editing the manuscript.

## References

- [1] R. Brooks, A.T. Horton and L. Torgesen, *J. Crystal Growth* 2 (1968) 279.
- [2] L.A. Monaco and F. Rosenberger, *J. Crystal Growth* (submitted).
- [3] F. Rosenberger, *J. Crystal Growth* 76 (1986) 618.
- [4] R.S. Feigelson, *J. Crystal Growth* 90 (1988) 1.
- [5] W. Ostwald, *Z. Physik. Chem.* 22 (1897) 302.
- [6] H.A. Miers and F. Isaac, *Proc. Roy. Soc. (London)* A79 (1907) 322.
- [7] J.W. Mullin and C. Gaska, *Cand. J. Chem. Eng.* 47 (1969) 483.
- [8] C. Thaller, G. Eichele, L.H. Weaver, E. Wilson, R. Karlson and J.N. Jansonius, in: *Methods in Enzymology*, Vol. 114, Eds. H.W. Wyckoff, C.H.W. Hirs and S.N. Timasheff (Academic Press, Orlando, FL, 1985) p. 132.
- [9] E.A. Stura and I.A. Wilson, *J. Crystal Growth* 110 (1991) 270.
- [10] T.A. Nyce and F. Rosenberger, *J. Crystal Growth* 110 (1991) 52.
- [11] A. McPherson and P. Shlichta, *J. Crystal Growth* 90 (1988) 47.
- [12] E.I. Givagizov, M.O. Kliya, V.R. Melik-Adamyanyan, A.I. Grebenko, R.C. DeMattei and R.S. Feigelson, *J. Crystal Growth* 112 (1991) 758.
- [13] A. McPherson, *Preparation and Analysis of Protein Crystals* (Wiley, New York, 1982)
- [14] A. McPherson, in: *Methods in Enzymology*, Vol. 114, Eds. H.W. Wyckoff, C.H.W. Hirs and S.N. Timasheff (Academic Press, Orlando, FL, 1985) p. 127.
- [15] L.J. Wilson, T.L. Bray and F.L. Suddath, *J. Crystal Growth* 110 (1991) 142.
- [16] F. Rosenberger and E.J. Meehan, *J. Crystal Growth* 90 (1988) 74.
- [17] H. Ritthausen, *J. prakt. Chem.* 23 (1881) 481.
- [18] T.B. Osborne, *Am. Chem. J.* 14 (1892) 662.
- [19] D.C. Hodgkin, *Cold Spring Harbor Symp. Quant. Biol.* 14 (1949) 65.
- [20] G.M.J. Schmidt, D.C. Hodgkin and B.M. Oughton, *Biochem. J.* 65 (1957) 744.
- [21] M.V. King, *J. Mol. Biol.* 1 (1959) 375.
- [22] J.S. Loehr, K.N. Mayerhoff, L.C. Sieker and L.H. Jensen, *J. Mol. Biol.* 91 (1975) 521.

- [23] A. Solomon, C.L. McLaughlin, C.H. Wei and J.R. Einstein, *J. Biol. Chem.* 245 (1970) 4975.
- [24] M. Zeppezauer, in: *Methods in Enzymology*, Vol. 22, Ed. W.B. Jakoby (Academic Press, New York, 1971) p. 253.
- [25] A.A. Green, *J. Biol. Chem.* 93 (1931) 495 and 517.
- [26] A.A. Green, *J. Biol. Chem.* 95 (1932) 47.
- [27] T.L. Blundell and L.N. Johnson, *Protein Crystallography* (Academic Press, New York 1976) p. 65.
- [28] G.S. Adair, *Proc. Roy. Soc (London)* A120 (1928) 573.
- [29] A.W. Hanson, M.L. Applebury, J.E. Coleman and H.W. Wyckoff, *J. Biol. Chem.* 245 (1970) 4975.
- [30] S. Hirono, K.T. Nakamura, Y. Iitaka and Y. Mitsui, *J. Mol. Biol.* 131 (1979) 855.
- [31] G. Gilliland and D.M. Bickham, *NIST/CARB Biological Macromolecule Crystallization Database* (U.S. Dept. Comm./NIST, Gaithersburg, MD, 1989).
- [32] F. Rosenberger, T. Nyce, E.J. Meehan, J.W. Sowers and L.A. Monaco, *Final Report NASA Grant NAG8-711* (1989).
- [33] R.S. Feigelson and R.C. DeMattei, paper presented at the Fourth International Conference on Crystal Growth of Biological Macromolecules, August 18-24 (1991) Freiburg, Germany.
- [34] S.B. Howard, P.J. Twigg, J.K. Baird and E.J. Meehan, *J. Crystal Growth* 90 (1988) 94.
- [35] M. Ataka and M. Asai, *J. Crystal Growth* 90 (1988) 86.
- [36] M.L. Pusey and K.G. Gernert, *J. Crystal Growth* 88 (1988) 419.
- [37] E. Cacioppo, S. Munson and M.L. Pusey, *J. Crystal Growth* 110 (1991) 66.
- [38] M.L. Pusey and S. Munson, *J. Crystal Growth* 113 (1991) 385.
- [39] E. Cacioppo and M.L. Pusey, *J. Crystal Growth* 114 (1991) 286.
- [40] R.C. DeMattei and R.S. Feigelson, *J. Crystal Growth* 110 (1991) 34.
- [41] V. Mikol and R. Giegé, *J. Crystal Growth* 97 (1989) 324.

- [42] A.J. Sophianopoulos, C.K. Rhodes, D.N. Holcomb and K.E. Van Holde, *J. Biol. Chem.* 237 (1962) 1107.
- [43] E. J. Meehan, private communication.
- [44] E.J. Cohn, F.R.N. Gurd, D.M. Surgenor, B.A. Barnes, R.K. Borwn, G. Derouaux, J.M. Gillespie, F.W. Kahnt, W.F. Lever, C.H. Liu, D. Mittelman, R.F. Mouton, K. Schmid and E. Uroma, *J. Am Chem. Soc.* 72 (1950) 465.
- [45] T.L. McMeekin, *J. Am. Chem. Soc.* 61 (1939) 2884.
- [46] E.J. Cohn, T.L. McMeekin, J.L. Oncley, J.M. Newell and W.L. Hughes, *J. Am. Chem. Soc.* 62 (1940) 3386.
- [47] E.J. Cohn, *Chem. Rev.* 28 (1941) 395.
- [48] J. Janatova, *J. Med.* 5 (1974) 149.
- [49] T. Arakawa and S.N. Timasheff, in: *Methods in Enzymology*, Vol. 114, Eds. H.W. Wyckoff, C.H.W. Hirs and S.N. Timasheff (Academic Press, Orlando, FL, 1985) p. 49.
- [50] S.C. Smith, S. Johnson, J. Andrews and A. McPherson, *Plant Physiology* 70 (1982) 1199.
- [51] A. McPherson and R. Spencer, *Arch. Biochem. Biophys.* 169 (1975) 650.
- [52] R.C. DeMattei and R.S. Feigelson, *J. Crystal Growth* 97 (1989) 333.
- [53] G.N. Phillips, Jr., in: *Methods in Enzymology*, Vol. 114, Eds. H.W. Wyckoff, C.H.W. Hirs and S.N. Timasheff (Academic Press, Orlando, FL, 1985) p. 128.

## Figure Captions

- Fig. 1. UV absorption spectrum of solution of 1.79 mg/ml horse serum albumin solution with 0.05 M acetate buffer, pH = 5.5.
- Fig. 2. Absorbance vs. concentration for horse serum albumin solutions with 0.05 M acetate buffer, pH = 5.5.
- Fig. 3. Scintillation arrangement for solubility studies, exploded view. See text for explanation.
- Fig. 4. Temperature trace and corresponding photodiode signal during initial, manually imposed nucleation and crystallite growth in scintillation experiment with 50 mg/ml lysozyme solution at 2.5 (w/v)% NaCl and pH = 4.5.
- Fig. 5. Temperature trace and corresponding photodiode signal during automatically controlled redissolution of crystallites in scintillation experiment with 11.1 mg/ml lysozyme solution at 2.1 (w/v)% NaCl and pH = 4.5.
- Fig. 6. Temperature dependence of solubility of lysozyme in solutions with pH = 4.5 and various salt concentrations. Symbols: experimental data; solid curves: polynomial fits, see table 1; dashed curves: results obtained by Pusey et al. [39] at 2.0 (w/v)% NaCl (upper curve) and 3.0 (w/v)% NaCl (lower curve).
- Fig. 7. Temperature dependence of solubility of horse serum albumin in solutions with pH = 5.5 and various ammonium sulfate concentrations. Symbols: experimental data; solid curves: polynomial fits, see table 2.
- Fig. 8. Experimental arrangement for the temperature-controlled growth of protein crystals in x-ray capillaries; cross-sectional view.
- Fig. 9. Lysozyme single crystal grown by dynamic temperature control in x-ray capillary.
- Fig. 10. Horse serum albumin single crystal grown by dynamic temperature control in x-ray capillary.

Table 1:

Third order polynomial fits to Lysozyme solubility data in  $\text{mg/ml} = A + BT + CT^2 + DT^3$  with  $T$  [ $^{\circ}\text{C}$ ].

NaCl (w/v)%	A	B	C x 10	D x 10 <sup>3</sup>	Avg. Dev. %
2.1	-58.8	9.18	-4.37	8.72	2.5
2.5	-55.1	9.31	-4.95	9.59	0.6
3.0	-215.4	27.7	-11.8	17.5	0.8

Table 2:

Fifth order polynomial fits to ESA solubility data in  $\text{mg/ml} = A + BT + CT^2 + DT^3 + ET^4 + FT^5$  with  $T [^{\circ}\text{C}]$ .

Am. Sulf. wt%	A	B	C	D x 10	E x 10 <sup>3</sup>	F x 10 <sup>5</sup>	Avg. Dev. %
45	57.9	7.82	-2.07	1.39	-3.75	3.36	0.7
47	92.1	-23.5	2.76	-1.63	4.66	-5.10	0.7
51	51.8	6.98	-2.46	2.08	-7.15	8.74	2.8

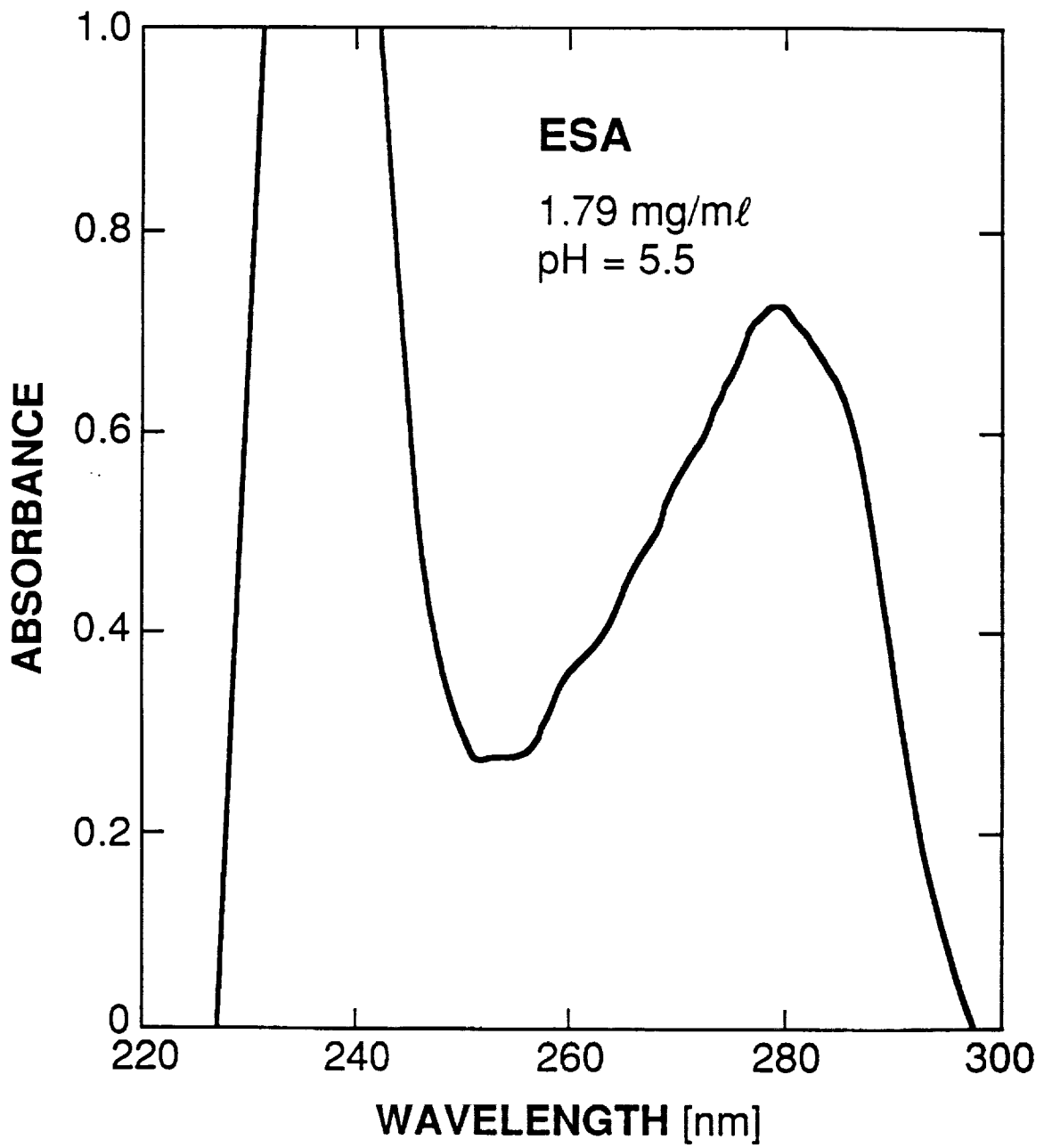


FIG. 1

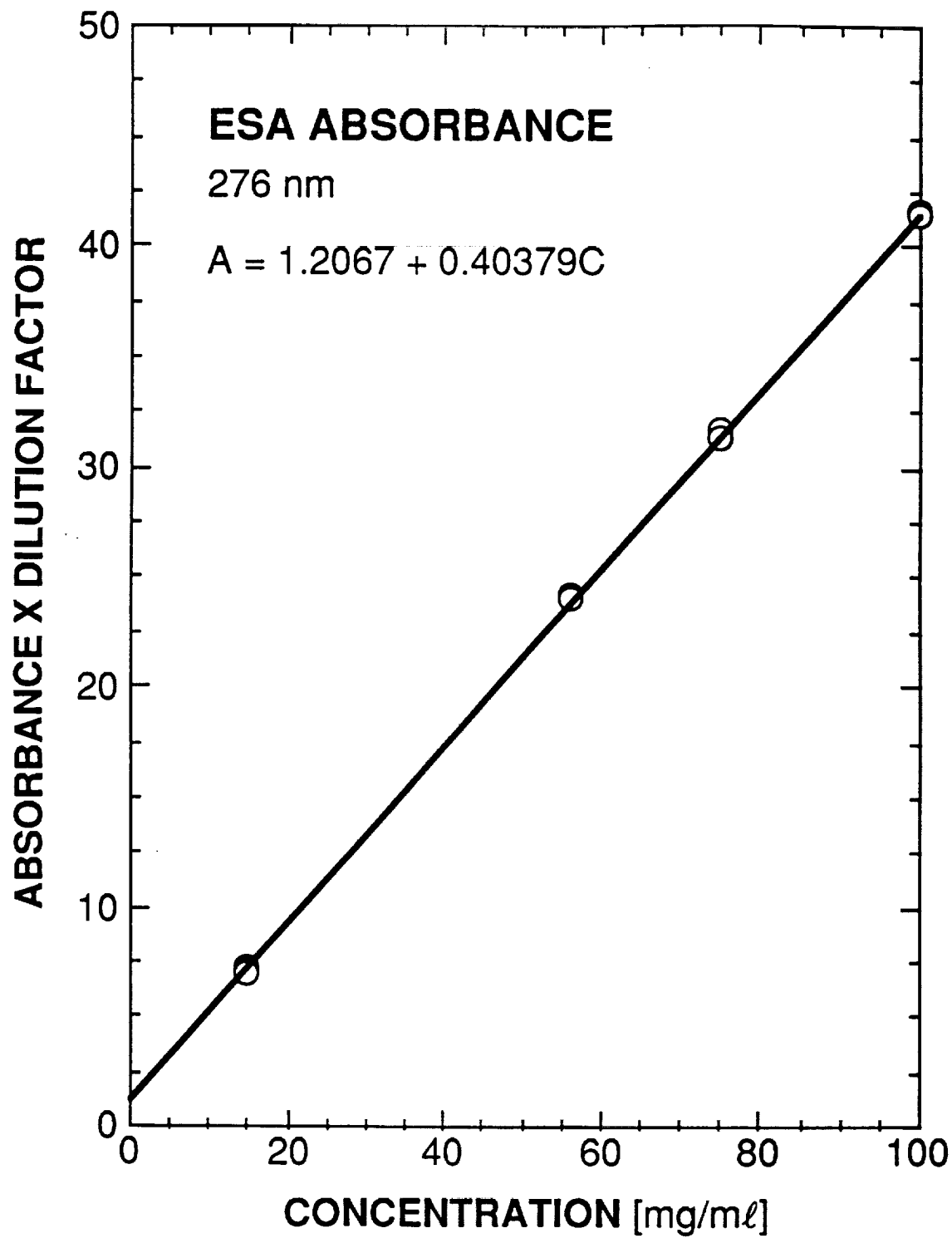


FIG. 2

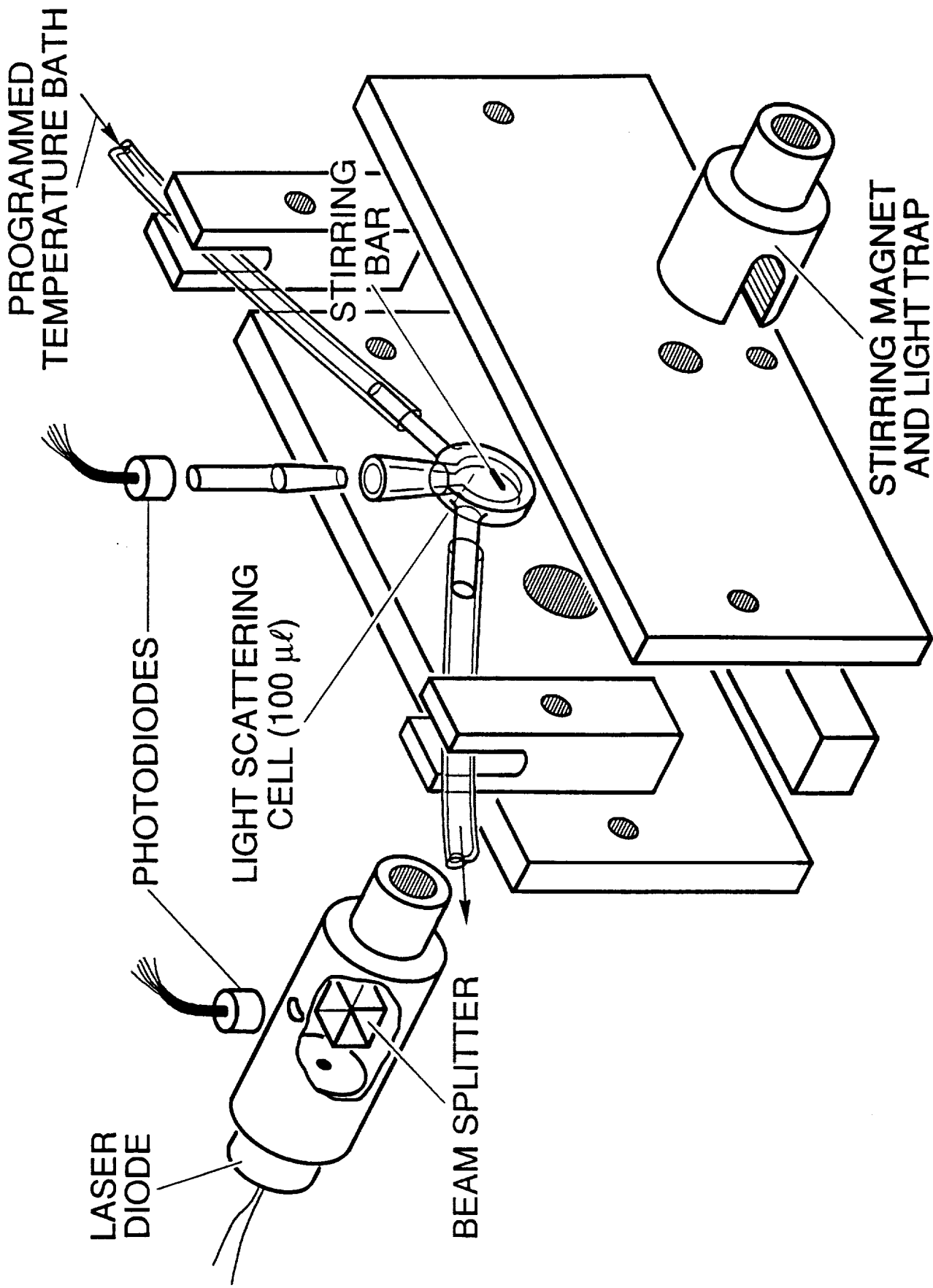


FIG. 3

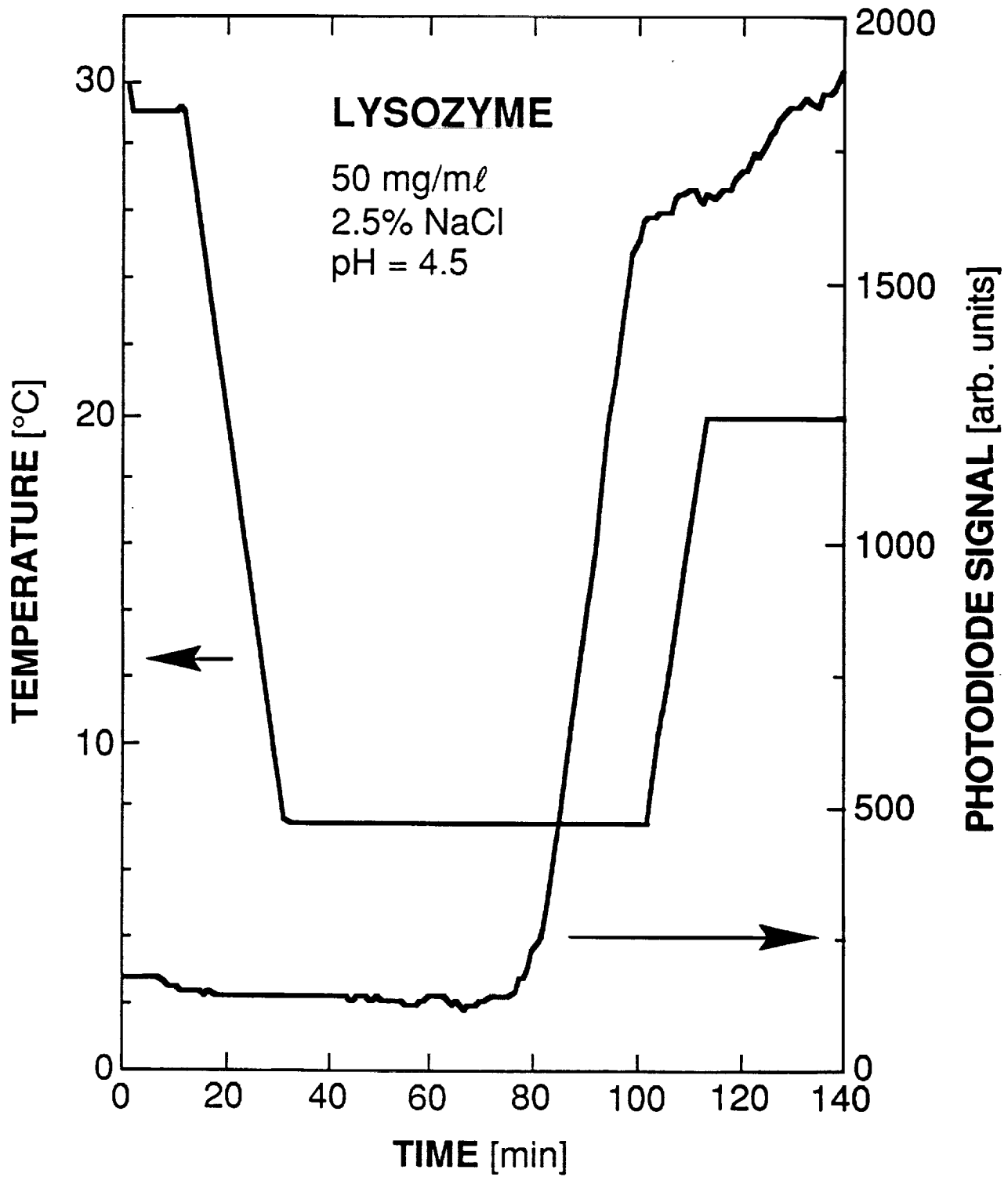


FIG. 4

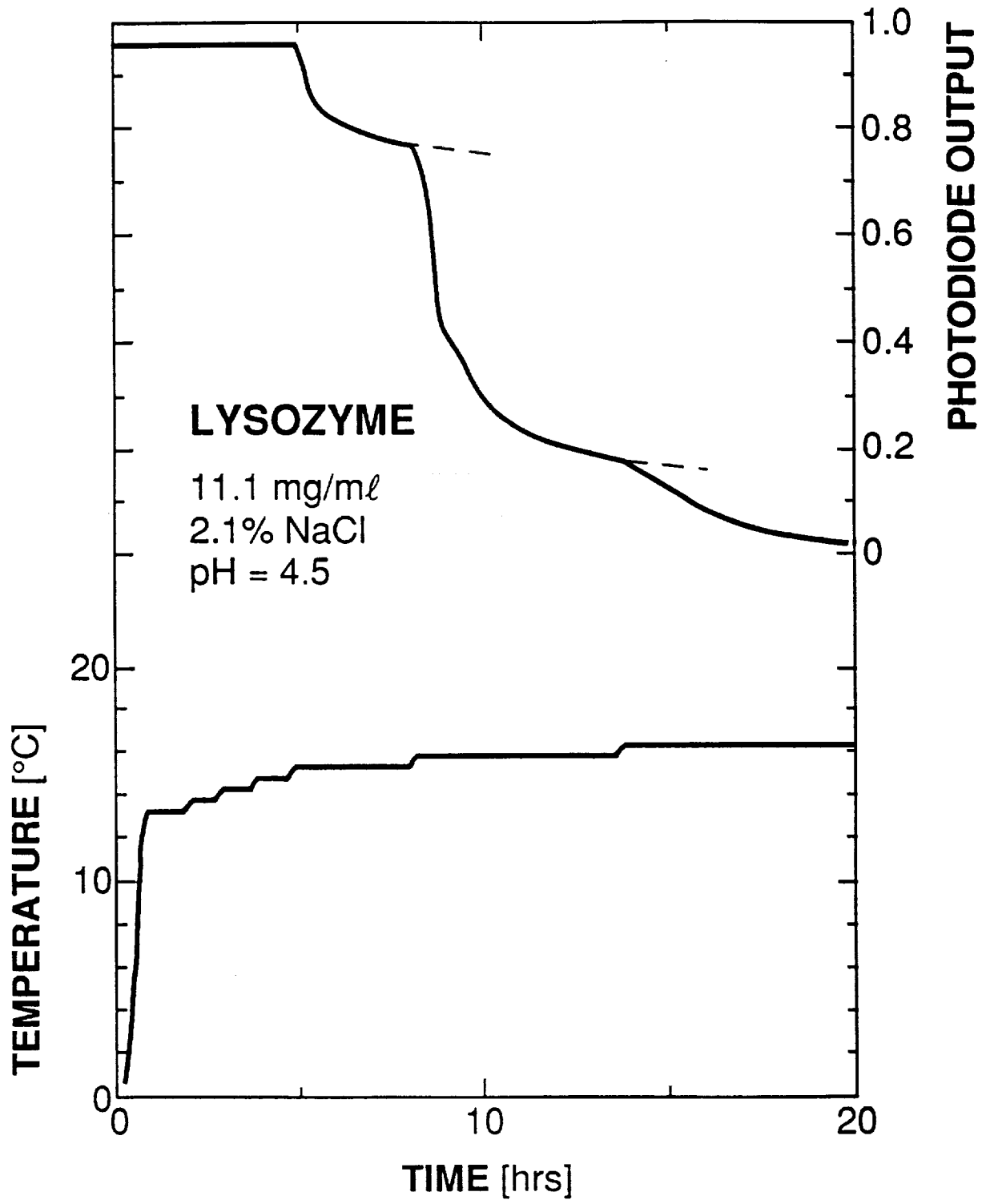


FIG. 5

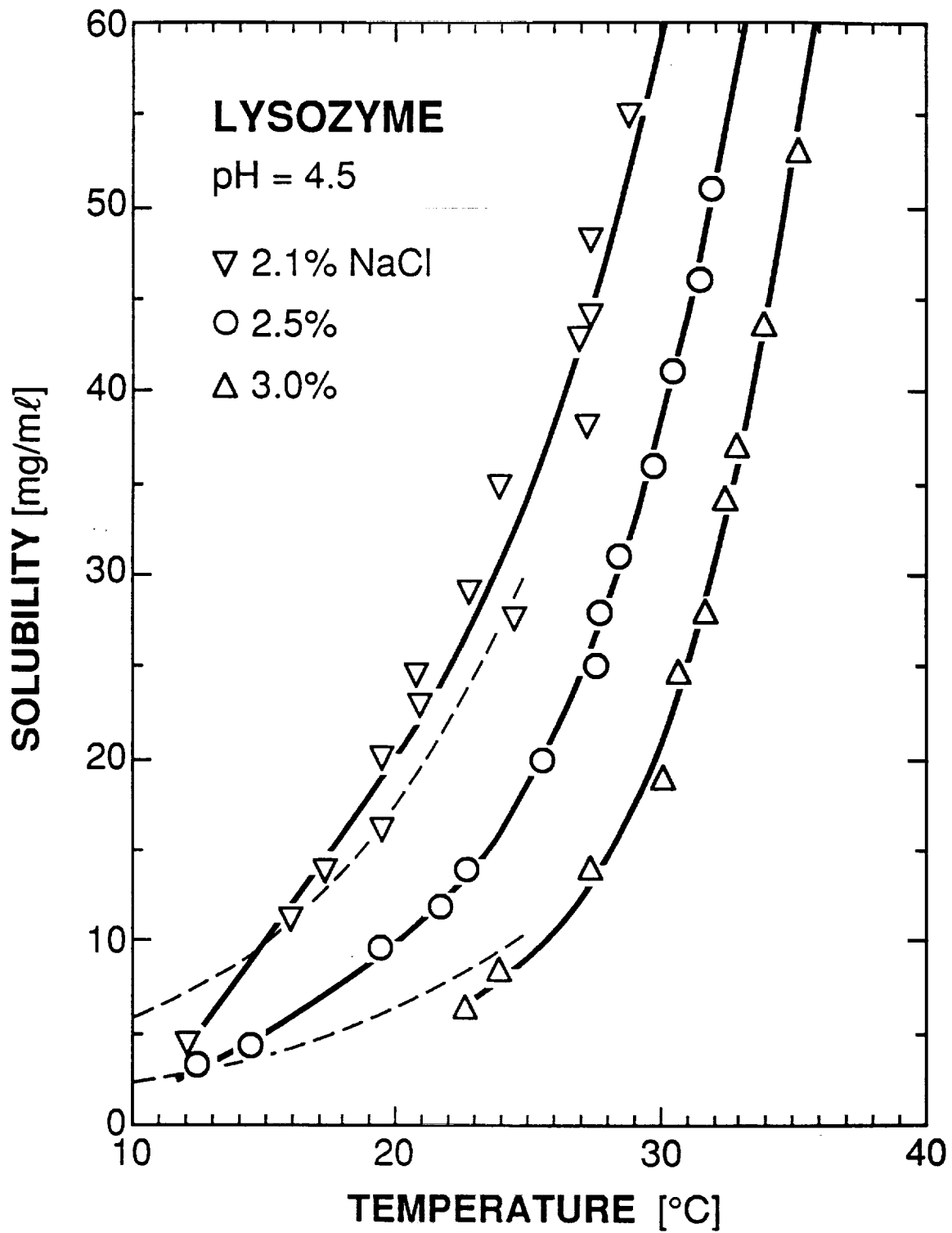


FIG. 6

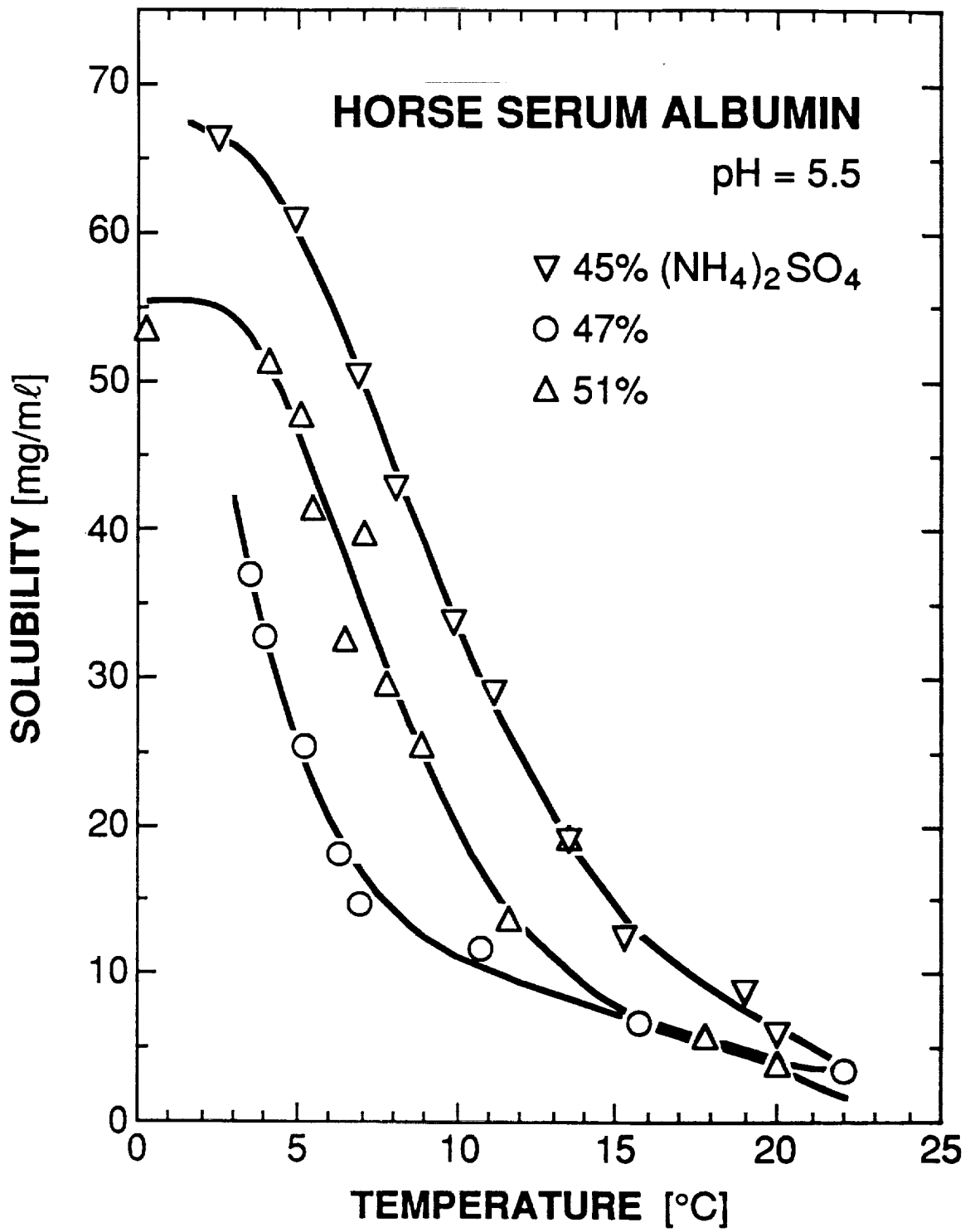


FIG. 7

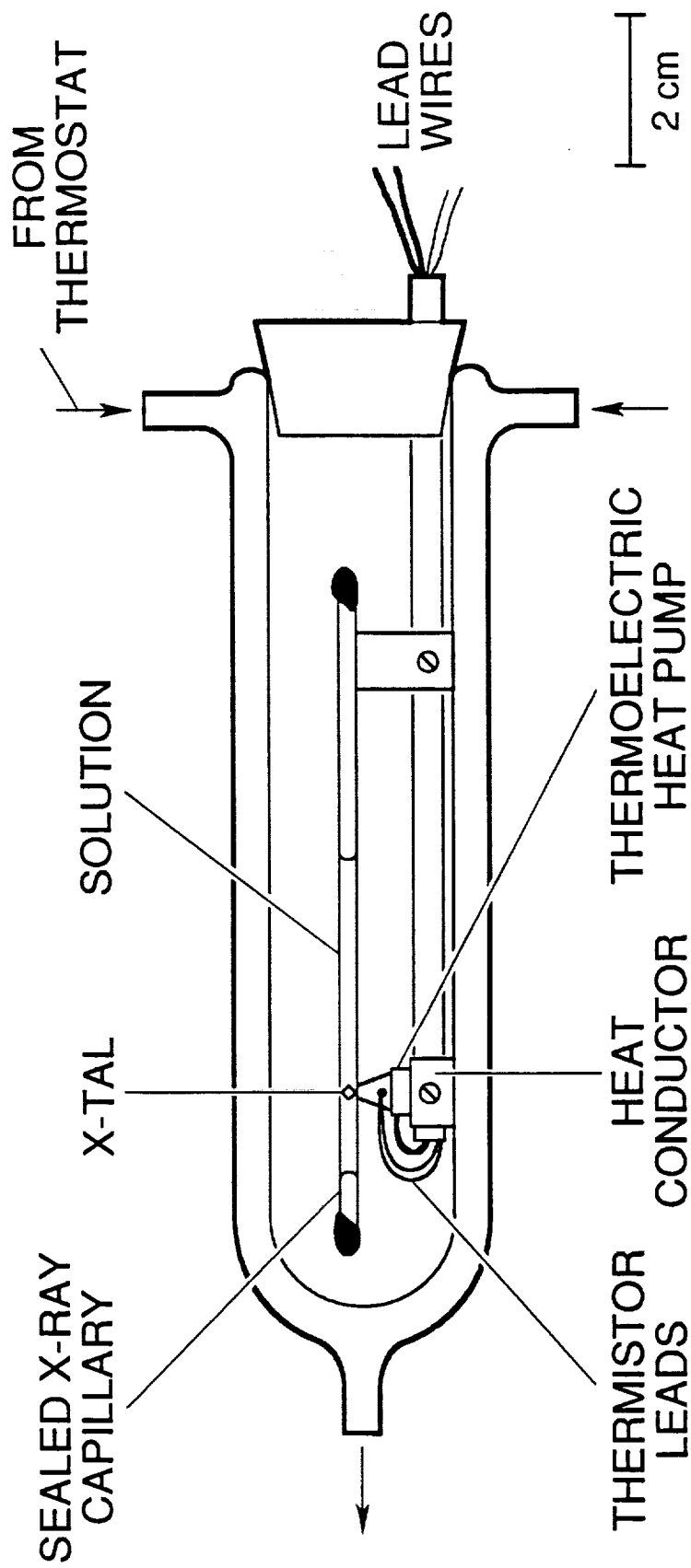


FIG. 8